



---

*Research article*

# **Influence of infill patterns and densities on the fatigue performance and fracture behavior of 3D-printed carbon fiber-reinforced PLA composites**

**Lubna Layth Dawood\* and Ehsan Sabah AlAmeen**

Department of Mechanical Engineering, Mustansiriyah University, Baghdad, Iraq

\* **Correspondence:** Email: [lubna.layth@uomustansiriyah.edu.iq](mailto:lubna.layth@uomustansiriyah.edu.iq); Tel: +964-770-22-45-307.

**Abstract:** This paper studied the mechanical properties of carbon fiber-reinforced polylactic acid (CF-PLA) samples manufactured with three different 3D-printed patterns: gyroid, tri-hexagon, and triangular. Filler content was generated in the samples at infill ratios of 30%, 60%, and 90%. Conventional tensile, flexural, impact, and fatigue tests were conducted to investigate the mechanical properties. It was found that the gyroid infill pattern enhanced performance, exhibiting tensile strength and modulus of elasticity up to 63% and 13% greater, respectively, than the tri-hexagon pattern at a 90% infill ratio. The fatigue life improvement was 113% compared with the tri-hexagon pattern. The tensile strength and modulus of elasticity increased up to 35% and 40% after including carbon fibers. The increase in flexural modulus was 30% compared to the triangular pattern, whereas impact energy absorption reached the best result with the triangular pattern, up to 89% more than the gyroid pattern. These results elucidate the optimization of infill patterns and ratios together with carbon fiber reinforcement for the development of CF-PLA components as a high-performance 3D printing solution for a wide range of engineering applications.

**Keywords:** PLA; CF; tri-hexagon; infill ratio; printing patterns; fatigue test

---

## **1. Introduction**

Additive manufacturing (AM), commonly known as 3D printing, is a transformative manufacturing process that constructs objects layer by layer from digital models [1,2]. This approach is fundamentally different from traditional manufacturing methods such as casting, molding, and machining [3,4], which often involve subtractive processes or significant tooling. AM offers

unparalleled versatility, flexibility, and customization, making it particularly suitable for a wide range of industrial applications, including biomedical devices, aerospace components, construction materials, and protective structures. The ability to produce complex geometries with high accuracy has led to the rapid adoption and development of 3D printing technology [5,6]. Fatigue properties are important for materials used in construction applications, especially under cyclic loading conditions [7]. Polylactic acid (PLA), a popular material for 3D printing due to its biodegradability and ease of use, exhibits different fatigue characteristics depending on printing parameters such as infill pattern, density, and process settings.

Research has shown that infill patterns play an important role in the fatigue performance of 3D-printed PLA [8]. The gyroid pattern, characterized by its continuous and smooth surface, tends to distribute stress more evenly, thereby enhancing fatigue resistance [9]. In comparison, other patterns like triangular and grid structures can create stress concentrations that may reduce fatigue life. Infill density, or the ratio of the printed material volume to the total volume, is another critical factor. Jap et al. demonstrated that different infill densities significantly influence the fatigue performance of 3D-printed PLA parts. Higher infill densities were found to enhance fatigue resistance, making the components more suitable for applications requiring durability under cyclic loading conditions. Higher infill densities generally improve the fatigue properties of 3D-printed PLA parts. This is because a denser infill reduces the presence of internal voids, which can act as initiation sites for fatigue cracks [10]. Studies by [11,12] support the finding that increasing the infill density from 20% to 80% significantly enhances the fatigue life of PLA components.

Process parameters such as layer height, print speed, and nozzle temperature also impact the fatigue resistance of 3D-printed PLA. Lower layer heights can improve the fatigue life by providing a smoother surface finish and better layer adhesion. Conversely, higher print speeds might reduce fatigue resistance due to insufficient inter-layer bonding [13]. Proper optimization of these parameters is crucial for achieving the desired fatigue performance. Comparative studies indicate that while the gyroid pattern typically offers superior fatigue resistance, the optimal choice of infill pattern and density can vary depending on the specific application and loading conditions. For instance, applications requiring a balance between weight and mechanical performance might benefit more from a tri-hexagon pattern with moderate infill density [14].

Fracture toughness measures a material's ability to resist crack propagation, crucial for maintaining the integrity of structural components. The effect of different infill patterns on the fracture toughness of PLA has been investigated; it was found that the gyroid pattern provided the highest fracture toughness among the patterns studied, including gyroid, tri-hexagon, and triangular [15]. This pattern's continuous and interconnected 3D lattice structure helps distribute stress more evenly, reducing the likelihood of crack initiation and propagation [16]. Roberts et al. supported these findings, showing that higher infill densities lead to improved fracture toughness. They observed that patterns like gyroid and tri-hexagon, when combined with higher infill densities, significantly enhance mechanical properties, including fracture toughness. Similarly, [16] demonstrated that the gyroid pattern's superior load distribution capabilities make it ideal for applications requiring high fracture toughness [17].

A comprehensive study by [18] examined the mechanical performance of PLA samples with various infill patterns and densities. Their results revealed that the gyroid pattern consistently offered superior mechanical performance, including higher strength and toughness, compared with other patterns like honeycomb and triangular. The gyroid pattern's continuous and interconnected structure

promotes better load distribution and reduces stress concentrations, leading to enhanced mechanical properties [19]. A systematic review by [19] analyzed the mechanical properties of different infill patterns, including triangular, grid, and tri-hexagon. The study found that while the tri-hexagon pattern showed improved compression strength, the triangular pattern provided balanced mechanical properties suitable for various applications. Furthermore, Domingo-Espin et al. highlighted that the gyroid and tri-hexagon patterns significantly enhance mechanical performance due to their efficient load-bearing structures [20].

The infill ratio, or density, plays a crucial role in determining the mechanical properties of 3D-printed parts. Studies consistently show that increasing the infill ratio enhances both fatigue properties and fracture toughness [21]. It has been demonstrated that higher infill densities result in better fatigue resistance and overall strength, a finding critical for applications requiring mechanical robustness [20]. It was also found that samples with a 90% infill density exhibit the highest tensile strength and fracture toughness, regardless of the infill pattern used. This suggests that while the choice of infill pattern is important, the infill ratio is a critical factor in optimizing the mechanical properties of 3D-printed PLA parts [22]. Gomez-Gras et al. corroborated these findings, showing that higher infill ratios significantly improve tensile strength and fracture toughness across various infill patterns [23,24].

This paper presents a new study on the fatigue properties and mechanical properties of carbon-reinforced PLA samples fabricated using three different 3D-printing patterns and three infill ratios. Although previous studies have examined the mechanical properties available in 3D-printed PLA, throughout though these studies tend to be different infill. This paper focuses on the comparative analysis of fatigue life and crack toughness in structures using standardized testing methods and thorough testing methods den applied, this study provides valuable insights into the optimal 3D printing process for improving mechanical performance of PLA-based materials. The findings contribute to the development of natural materials and additive manufacturing Concepts and are these and provide useful explanations. This study investigates the influence of different infill patterns (gyroid, tri-hexagon, and triangular) and densities (30%, 60%, and 90%) on the fatigue performance and fracture behavior of 3D-printed carbon fiber-reinforced PLA (CF-PLA) composites. The selection of these specific infill patterns is particularly relevant due to their unique geometric properties, which can significantly influence the mechanical performance of the printed parts. For instance, the gyroid pattern, known for its continuous, smooth surfaces and minimal internal stress concentrations, is anticipated to enhance the structural integrity and fatigue resistance of the composites. The tri-hexagon and triangular patterns, on the other hand, offer distinct advantages in terms of load distribution and stiffness, making them ideal candidates for this comparative study.

## **2. Materials and methods**

### *2.1. Overview of experimental workflow*

The experimental workflow for this study is outlined in Figure 1. The process begins with material selection, followed by the 3D printing process, specimen preparation, mechanical testing, and data analysis. Each step is critical to ensure the reliability and accuracy of the results.

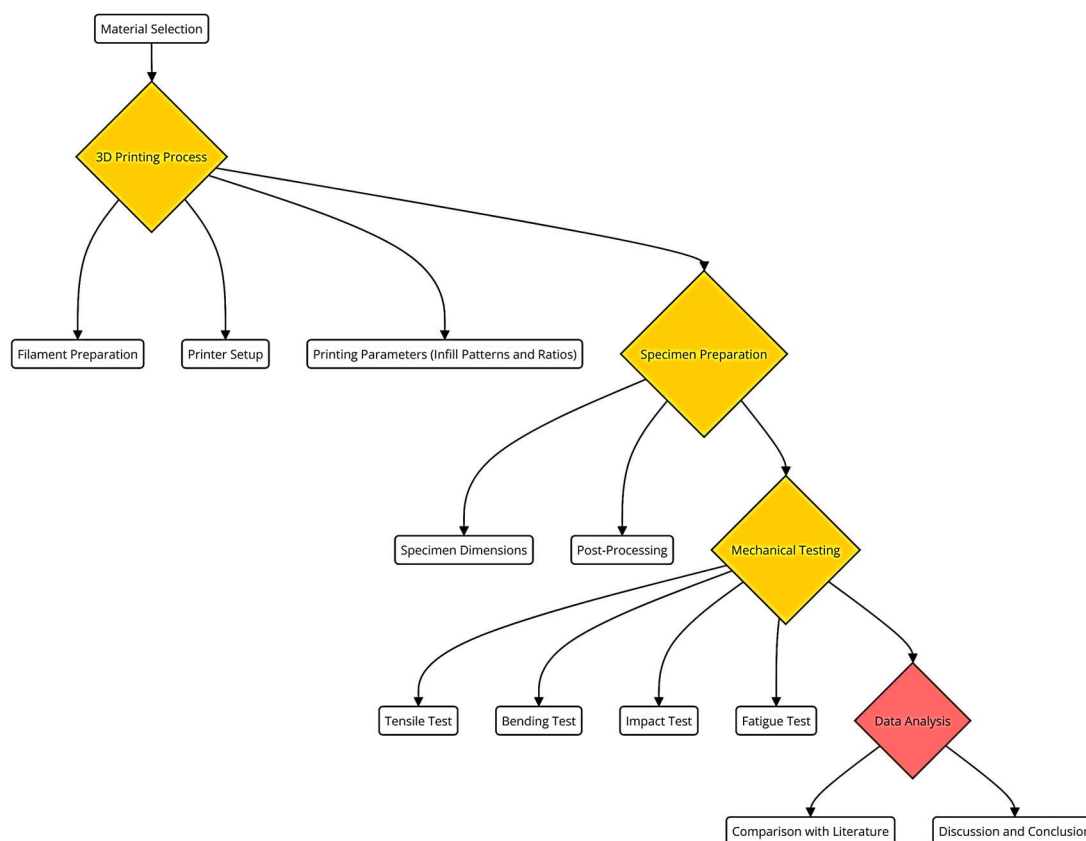


**Figure 1.** Experimental workflow.

**Material selection:** the first step involves selecting the appropriate material for the study, in this case, CF-PLA.

**3D printing process:** the 3D printing process includes filament preparation, printer setup, and setting the printing parameters, namely infill patterns (gyroid, tri-hexagon, and triangular) and infill ratios (30%, 60%, and 90%).

**Specimen preparation:** once printed, the specimens are prepared according to specific dimensions and may undergo post-processing to ensure they meet the required standards.

**Mechanical testing:** the prepared specimens are subjected to various mechanical tests, including tensile, bending, impact, and fatigue tests, to evaluate their performance.

**Data analysis:** the results from the mechanical tests are analyzed and compared with existing literature. This analysis helps in understanding the improvements in mechanical properties and the potential mechanisms behind them.

Each of these steps is detailed in the subsequent sections, providing a comprehensive understanding of the methodology employed in this study.

## 2.2. Materials and sample preparation

In this study, PLA filament was used as the base material for all 3D-printed samples. PLA was chosen due to its biodegradable nature, ease of use in 3D printing, and favorable mechanical properties. The PLA filament utilized had a diameter of 1.75 mm, and the 3D printing was conducted using a

fused deposition modeling (FDM) printer. Three distinct infill patterns were selected for comparison: gyroid, tri-hexagon, and triangular. These patterns were chosen based on their varied geometrical structures and potential to influence the mechanical properties of the printed samples, as shown in Figure 2. Each pattern was printed at three different infill ratios: 0%, 60%, and 90%. The choice of these ratios aims to provide a comprehensive analysis of the impact of infill density on mechanical properties, particularly focusing on fatigue life and fracture toughness.

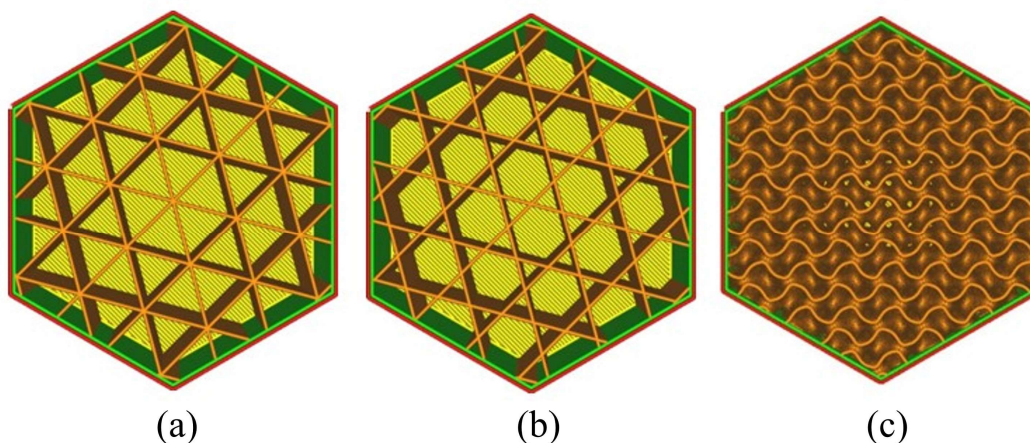


**Figure 2.** Infill patterns: (a) triangle; (b) tri-hexagon; (c) gyroid.

The printing parameters shown in Table 1 were standardized across all samples to ensure consistency. To address a reviewer's concern, a hardened nozzle with a diameter of 0.4 mm was used, which aligns with best practices for printing PLA with carbon fiber reinforcement. However, based on the literature recommendations, the layer height was adjusted to 0.3 mm to prevent defects and ensure optimal adhesion and mechanical properties. The printing temperature was set to 210 °C, the bed temperature to 60 °C, and the printing speed was maintained at 60 mm/s. These parameters were selected based on recommendations from previous studies to optimize the mechanical properties of PLA prints [1,2]. The samples were fabricated using a Creality Ender 3 Pro 3D printer, as shown in Figure 3.

**Table 1.** 3D printing parameters.

Parameter	Value
Filament diameter	1.75 mm
Printing temperature	210 °C
Bed temperature	60 °C
Nozzle diameter	0.4 mm
Layer height	0.2 mm
Printing speed	60 mm/s
Infill patterns	Gyroid, tri-hexagon, triangular
Infill ratios	30%, 60%, 90%

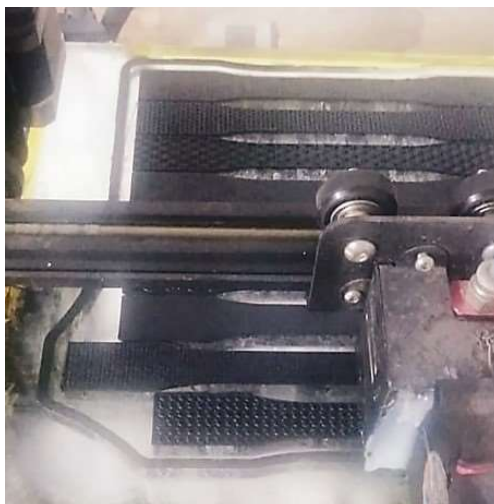


**Figure 3.** Manufacturing image of 3D printing.

### *2.3. Effect of carbon fiber reinforcement*

The incorporation of carbon fibers as a reinforcement material has been widely recognized for its ability to significantly enhance the mechanical properties of polymer matrices, including PLA. Carbon fibers possess exceptional strength and stiffness while maintaining low density, making them an ideal reinforcement material for improving the performance of PLA [1,2]. In this study, CF-PLA samples were prepared and compared against non-reinforced PLA samples to evaluate the influence of carbon fiber reinforcement on fatigue properties and fracture toughness. The CF-PLA samples were obtained by blending chopped carbon fibers with PLA filament during the 3D printing process, as shown in Figure 4a. This blending process ensures a uniform distribution of carbon fibers within the PLA matrix, facilitating efficient load transfer and enhancing the overall mechanical properties of the composite material. Figure 4a depicts the 3D printing setup used in this study. The yellow item indicates the filament spool, which feeds the PLA filament into the printer. The blue item is the filament guide, ensuring smooth delivery of the filament to the extruder. The black item represents the extruder, which heats and pushes the filament through the nozzle. The green item is the nozzle itself, where the heated filament is extruded to form the printed layers. This setup allows for precise control over the printing process, ensuring consistent reinforcement distribution in the CF-PLA samples. Figure 4b shows an scanning electron microscope (SEM) image of the chopped carbon fibers used for reinforcement, depicting their morphology and dimensions.

Numerous studies have demonstrated the beneficial effects of carbon fiber reinforcement on the mechanical properties of PLA. CF-PLA composites exhibit higher tensile strength, improved modulus of elasticity, and better thermal resistance compared with non-reinforced PLA [3,4]. The reinforcing effect of carbon fibers is attributed to their high strength-to-weight ratio, as well as their ability to effectively transfer loads from the polymer matrix, resulting in enhanced mechanical performance. By incorporating carbon fiber reinforcement, this study aims to investigate the potential improvements in fatigue properties and fracture toughness of 3D-printed PLA components. The comparison between CF-PLA and non-reinforced PLA samples will provide valuable insights into the role of carbon fiber reinforcement in enhancing the durability and crack resistance of 3D-printed structures.



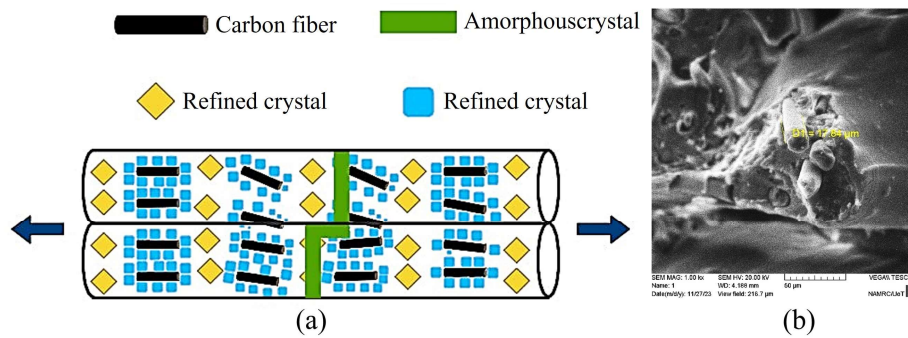


**Figure 4.** (a) Carbon fiber-reinforced PLA filament used for 3D printing; (b) SEM image of chopped carbon fibers used for reinforcement in the PLA matrix.

#### 2.4. Tensile testing

Tensile tests were conducted following the ASTM D638 Type IV standard to evaluate the tensile properties of the 3D-printed PLA samples. The tests were performed on a universal testing machine (UTM) equipped with a 10 KN load cell. Specimens with dimensions as shown in Figure 5 were subjected to uniaxial tensile loading at a constant crosshead speed of 5 mm/min until failure occurred [25,26]. The tensile properties measured included ultimate tensile strength, yield strength, and elongation at break.

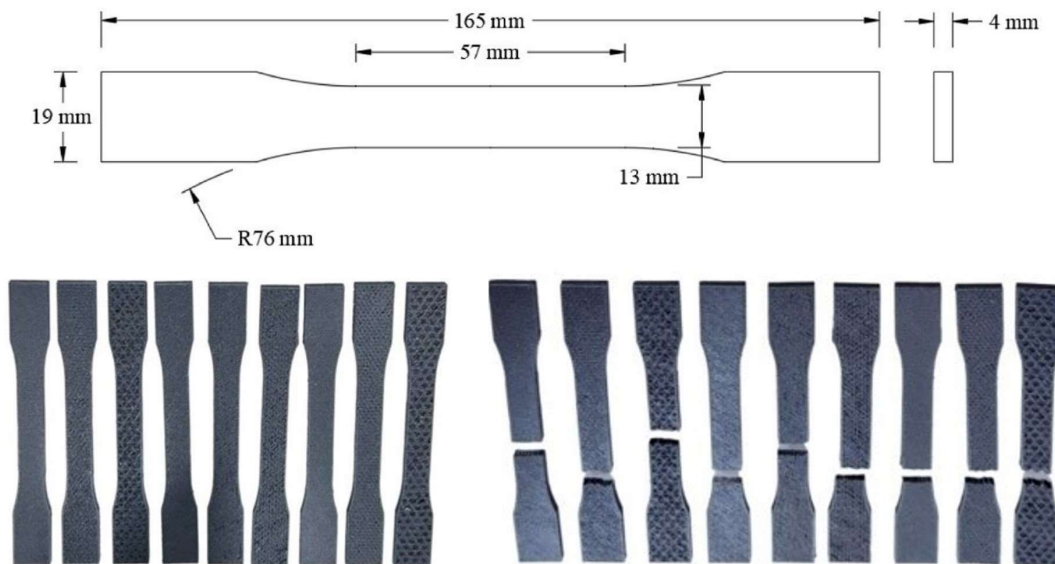


**Figure 5.** Dimensions of the tensile test specimen according to ASTM D638 Type IV standard.

## 2.5. Bending test

The flexural behavior of the material was evaluated through a three-point bending test conducted at room temperature [27–29]. The bending test specimens were designed in accordance with the ASTM D790 standard, with dimensions as shown in Figure 6. Specimens were manufactured with infill ratios of 30%, 60%, and 90%, and infill patterns of triangles, tri-hexagons, and gyroids. The test was performed using a Laryee tensile testing machine with a 50 KN load capacity, allowing for the determination of the flexural modulus.

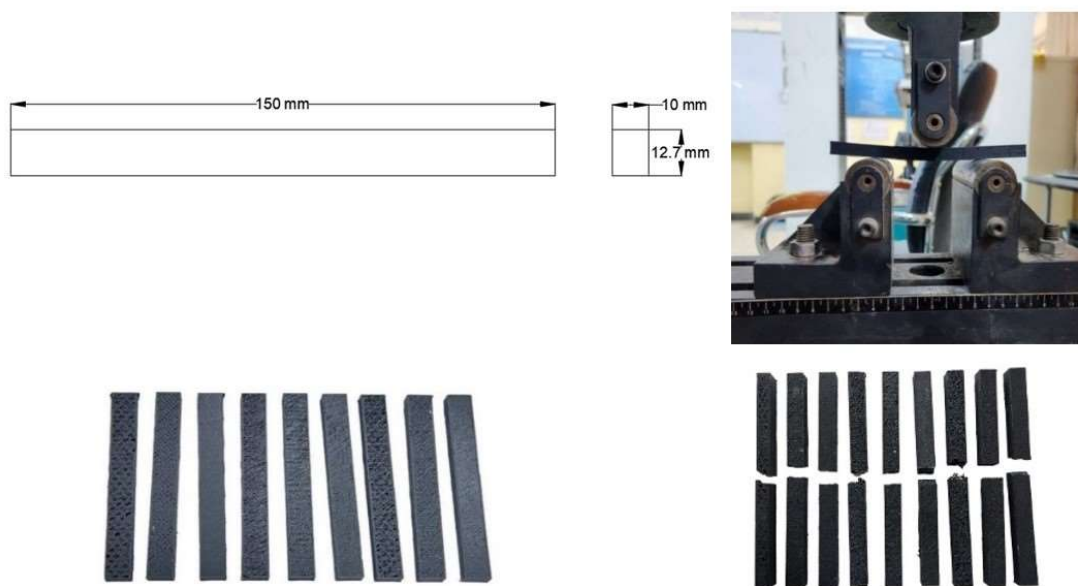


**Figure 6.** Dimensions of the bending test specimen according to ASTM D790 standard.

## 2.6. Fatigue test

Fatigue tests were performed to evaluate the endurance limit of the 3D-printed samples. The tests were conducted using a cyclic loading machine capable of applying sinusoidal loads, with dimensions as shown in Figure 7. The samples were subjected to repeated tensile-compressive cycles at a frequency of 5 Hz. The stress range for the fatigue tests was selected based on the tensile test results, typically set at 50% of the ultimate tensile strength of the material. The number of cycles to failure was recorded for each sample. Fatigue life was then analyzed to determine the influence of infill pattern and density on the material's durability under cyclic loading conditions [30,31].



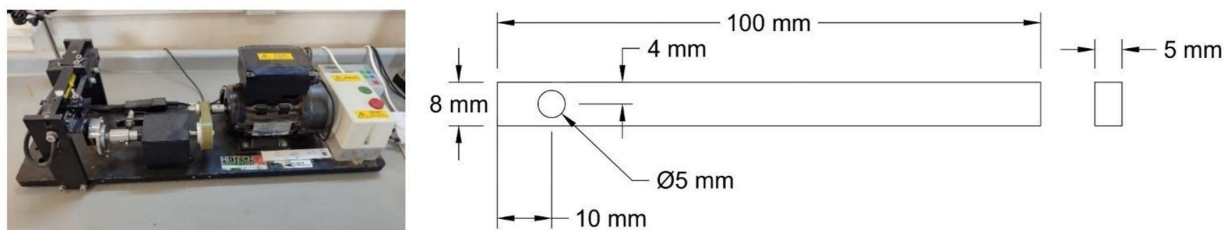


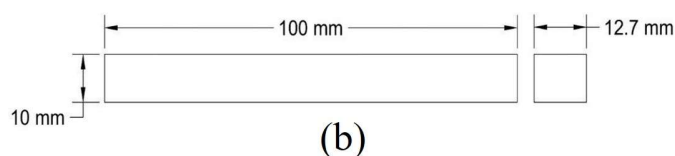
**Figure 7.** Fatigue testing machine used for evaluating the endurance limit.

### 2.7. Impact testing

The energy of impact was measured using a Tinius Olsen impact testing machine (Figure 8a) to evaluate the material's ability to absorb sudden loads and resist fracture. Impact testing provides valuable information about the material's toughness and its capacity to withstand dynamic loading conditions. The impact test results will shed light on the influence of infill patterns and ratios on the impact resistance of the 3D-printed PLA samples. The impact test specimens were designed according to the ASTM D6110 standard, with dimensions as depicted in Figure 8b. The specimens were fabricated with infill ratios of 30%, 60%, and 90%, and infill patterns of triangles and gyroids.



(a)



(b)

**Figure 8.** Impact test procedure.

### 2.8. Fracture toughness testing

The resistance of the material to crack propagation was assessed through fracture toughness tests conducted using single-edge notched bending (SENB) specimens. Fracture toughness is a critical property that determines the material's ability to resist crack growth and prevent catastrophic failure.

The fracture toughness test results will provide insights into the influence of infill patterns and ratios on the crack resistance of the 3D-printed PLA samples. The specimens were prepared in accordance with the ASTM D5045 standard. During the tests, the load-displacement data were recorded, enabling the calculation of the critical stress intensity factor (KIC), which provides a quantitative measure of the material's fracture toughness.

### 3. Results and discussion

#### 3.1. Tensile test results

The tensile properties of the carbon fiber-reinforced PLA samples were evaluated using the average results of three specimens for each combination of infill ratio and infill pattern, as presented in Table 2. Figures 9–11 illustrate the stress–strain relationships for the three infill patterns (gyroid, tri-hexagon, and triangle) at infill ratios of 30%, 60%, and 90%, respectively. At a 30% infill ratio (Figure 9), the gyroid pattern exhibited the highest ultimate stress value of 5.19 MPa, which was 40% and 12% higher than the tri-hexagonal and triangle patterns, respectively. Similarly, at a 60% infill ratio (Figure 10), the gyroid pattern demonstrated the maximum stress value of 9.42 MPa, surpassing the tri-hexagonal and triangle patterns by 79% and 33%, respectively. For the 90% infill ratio (Figure 11), the gyroid pattern again showed the highest ultimate stress value of 18.2 MPa, which was 63% and 58% higher than the tri-hexagonal and triangle patterns, respectively.

The superior tensile properties of the gyroid pattern can be attributed to the reinforcing effect of the carbon fibers, which serve as a load-bearing framework within the PLA matrix. The continuous and interconnected nature of the gyroid structure allows for efficient stress distribution and load transfer, leading to enhanced tensile strength [32].

**Table 2.** Tensile test results of the carbon fiber poly(lactic acid) carbon fiber-reinforced samples.

Specimen	Infill ratio (%)	Infill pattern	Modulus of elasticity (MPa)	Maximum stress (MPa)
L1	30	Tri-hexagon	320	3.72
L2	60	Tri-hexagon	589	5.26
L3	90	Tri-hexagon	881	11.2
L4	30	Gyroid	333	5.19
L5	60	Gyroid	730	9.42
L6	90	Gyroid	999	18.2
L7	30	Triangle	334	4.62
L8	60	Triangle	593	7.08
L9	90	Triangle	837	11.5

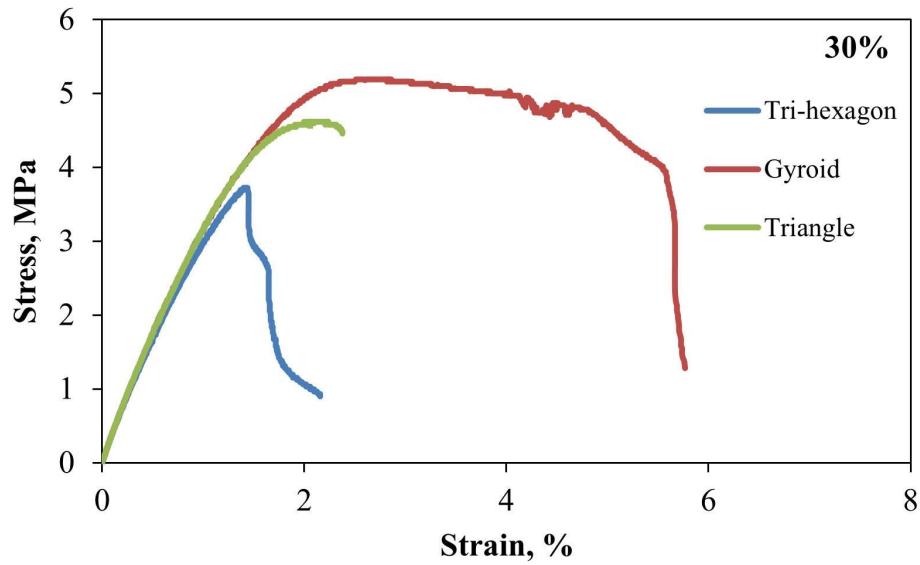


**Figure 9.** Stress-strain relation for the three patterns with 30% fill ratio.

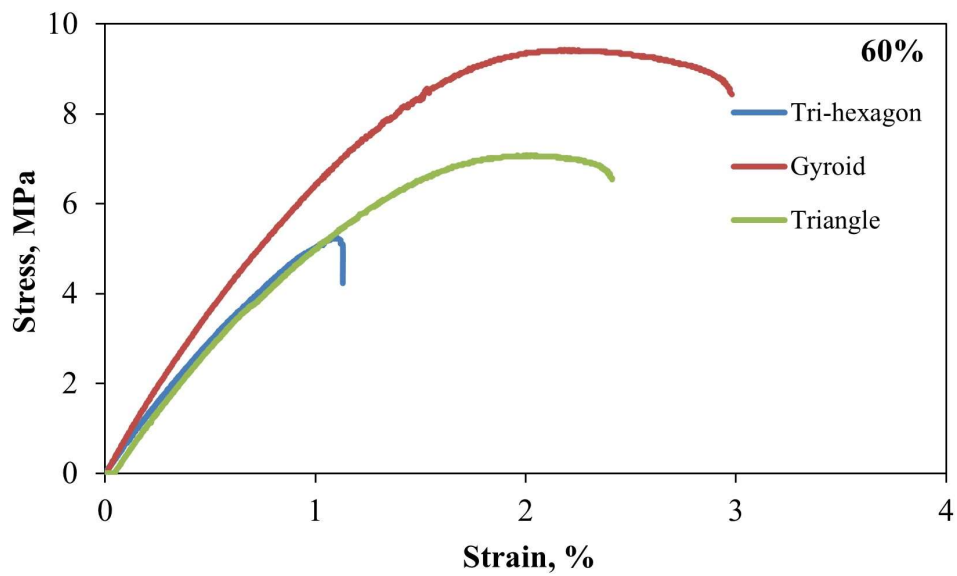


**Figure 10.** Stress-strain relationship for the three patterns with an infill ratio of 60%.

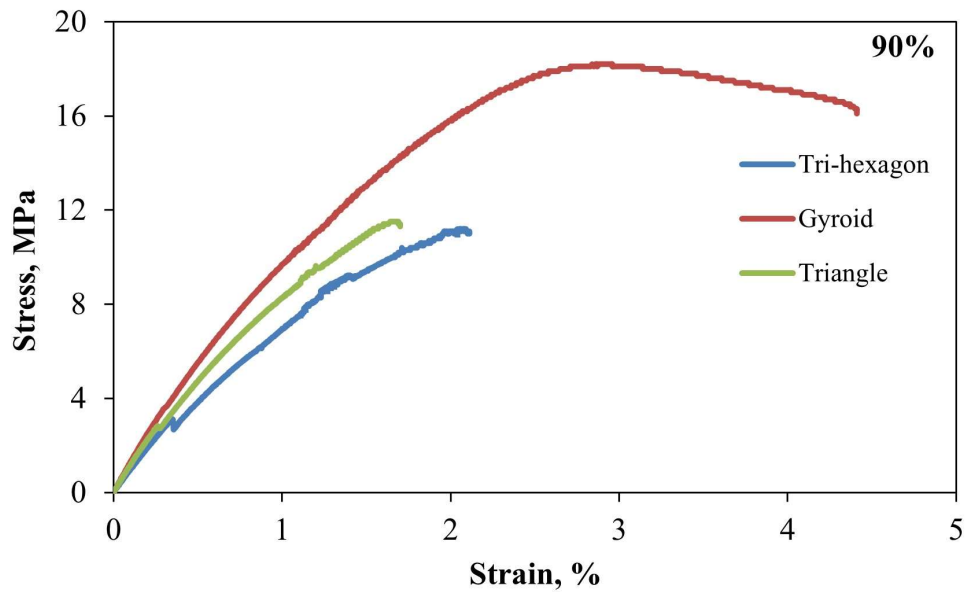


**Figure 11.** Stress-strain relationship for the three patterns with an infill ratio of 90%.

Figures 12–14 present the elastic modulus values for the three infill patterns at infill ratios of 30%, 60%, and 90%, respectively. At a 30% infill ratio (Figure 12), the triangle pattern exhibited the highest elastic modulus of 334 MPa, slightly surpassing the gyroid and tri-hexagon patterns by 0.3% and 4%, respectively. However, at higher infill ratios of 60% (Figure 13) and 90% (Figure 14), the gyroid pattern demonstrated superior elastic modulus values of 730 MPa and 999 MPa, respectively, outperforming the tri-hexagon and triangle patterns by 23%–24% and 13%–19%, respectively.

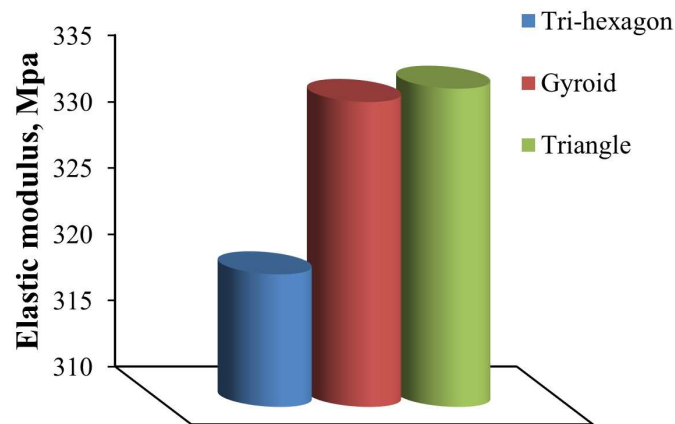


**Figure 12.** Elastic modulus (infill ratio 30%).

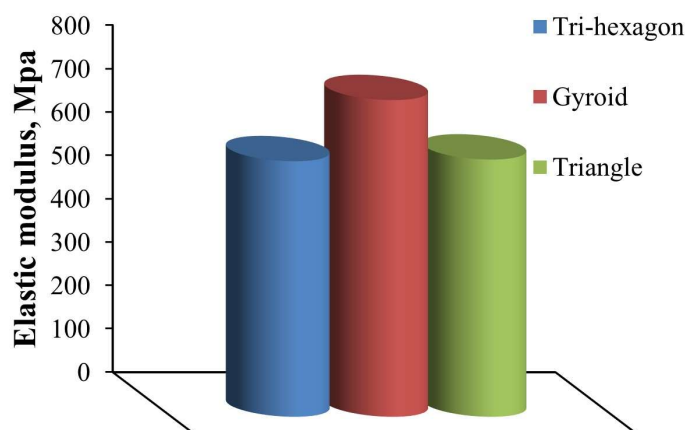


**Figure 13.** Elastic modulus (infill ratio 60%).

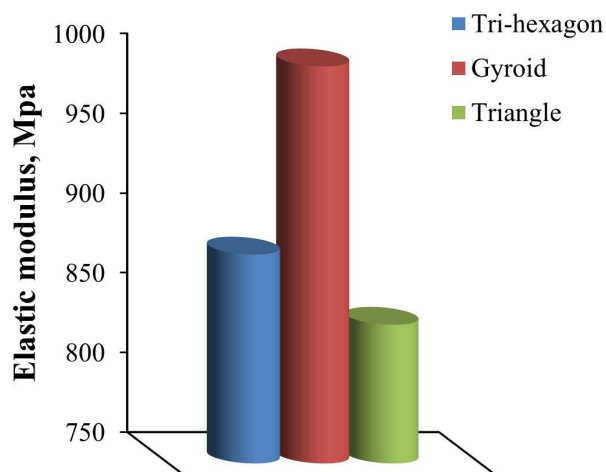


**Figure 14.** Elastic modulus (infill ratio 90%).

The effect of the infill ratio on the ultimate strength is evident, as shown in Figures 15–17. For the gyroid pattern (Figure 15), increasing the infill ratio from 30% to 60% resulted in an 82% increase in strength, while a further increase from 60% to 90% led to a 90% improvement. The tri-hexagon pattern (Figure 16) exhibited even greater sensitivity to infill ratio, with the 90% infill ratio sample showing a 113% higher ultimate strength compared to the 60% infill ratio sample.

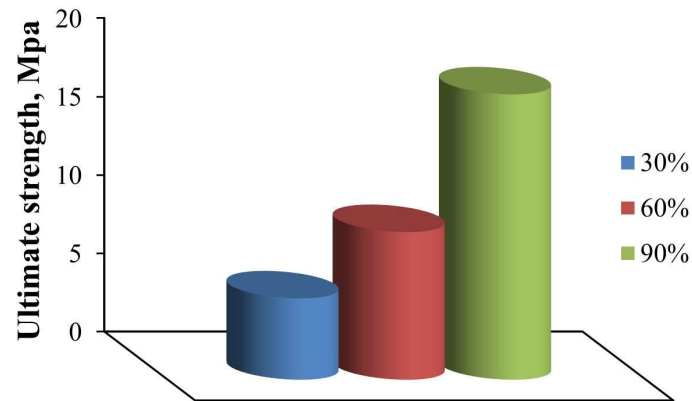


**Figure 15.** Ultimate strength (gyroid pattern).

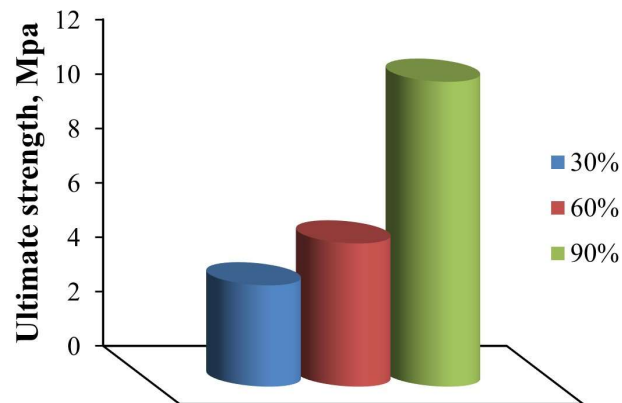


**Figure 16.** Ultimate strength (tri-hexagon pattern).

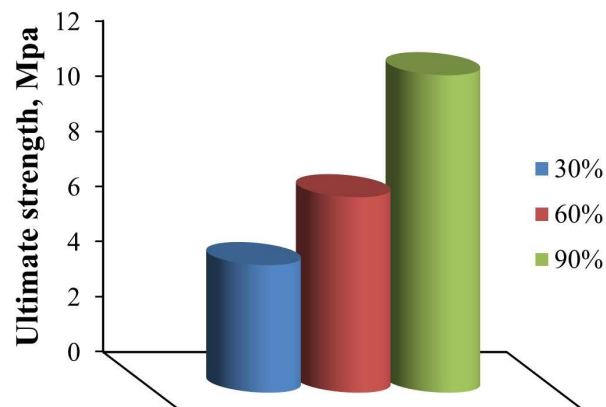


**Figure 17.** Ultimate strength (triangle pattern).

Figures 18–20 show a comparison of the elastic moduli for the three patterns (gyroid, tri-hexagon, and triangle) for the infill ratios of 30%, 60%, and 90%, respectively. Figures demonstrate that the gyroid pattern has the highest elastic modulus value for all infill ratios, indicating its superior stiffness.



The tri-hexagonal pattern has a lower elastic modulus value than the gyroid pattern, while the triangle pattern has the lowest elastic modulus value.

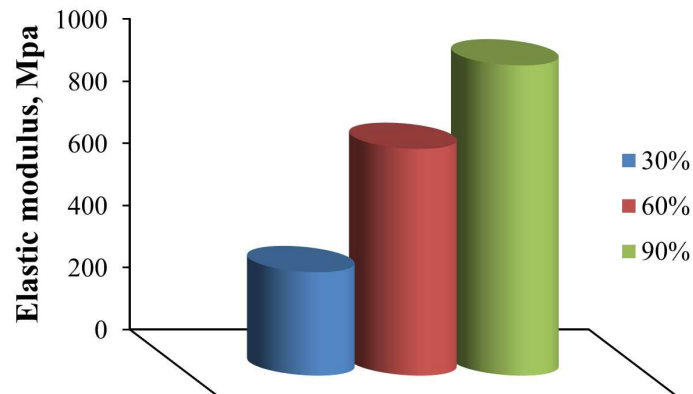


**Figure 18.** Elastic modulus (gyroid pattern).

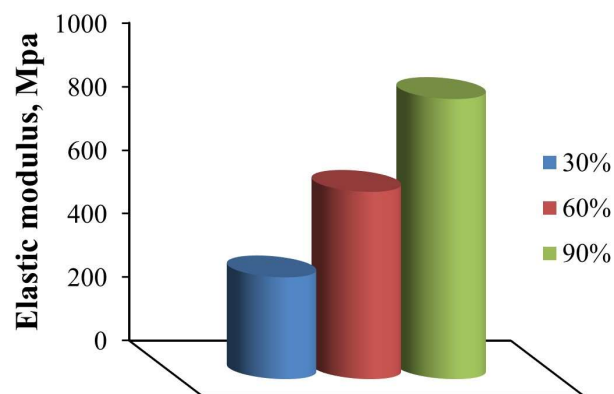


**Figure 19.** Elastic modulus (tri-hexagon pattern).

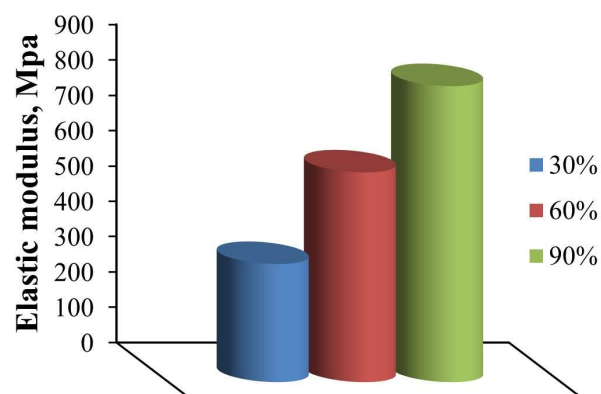


**Figure 20.** Elastic modulus (triangular pattern).

These findings are consistent with previous studies that have reported improved mechanical properties with increasing infill density in 3D-printed parts [20–22]. The higher infill ratios result in a denser material with fewer voids, allowing for better load distribution and enhanced mechanical performance.

### 3.2. Bending test results

The flexural modulus of the carbon fiber-reinforced PLA samples was determined using a three-point bending test. Twenty-seven specimens were tested with three infill ratios (30%, 60%, and 90%) and three infill patterns (tri-hexagon, gyroid, and triangle). The average flexural modulus values for each specimen are presented in Table 3. The gyroid pattern at a 90% infill ratio exhibited the highest flexural modulus of 1242 MPa. This superior performance can be attributed to the gyroid pattern's ability to distribute stresses more efficiently, combined with the reinforcing effect of the carbon fibers [17,18].

**Table 3.** Values of flexural modulus for bending test.

Specimen code	Flexural modulus (MPa)
TH 30	123
TH 60	464
TH 90	957
G 30	291
G 60	660
G 90	1242
TR 30	265
TR 60	572
TR 90	1049

### 3.3. Impact test results

Impact tests were conducted on 27 samples with varying infill ratios and patterns to determine the energy of impact and calculate the fracture toughness. The results, summarized in Table 4, indicate that the triangle pattern exhibited the highest energy absorption, followed by the gyroid pattern. The superior impact resistance of the triangle pattern can be explained by its geometry, which allows for effective dissipation of impact energy through the interconnected triangular structure [19]. The gyroid pattern's good impact performance is attributed to its continuous and smooth surface, which helps distribute stresses more evenly [16].

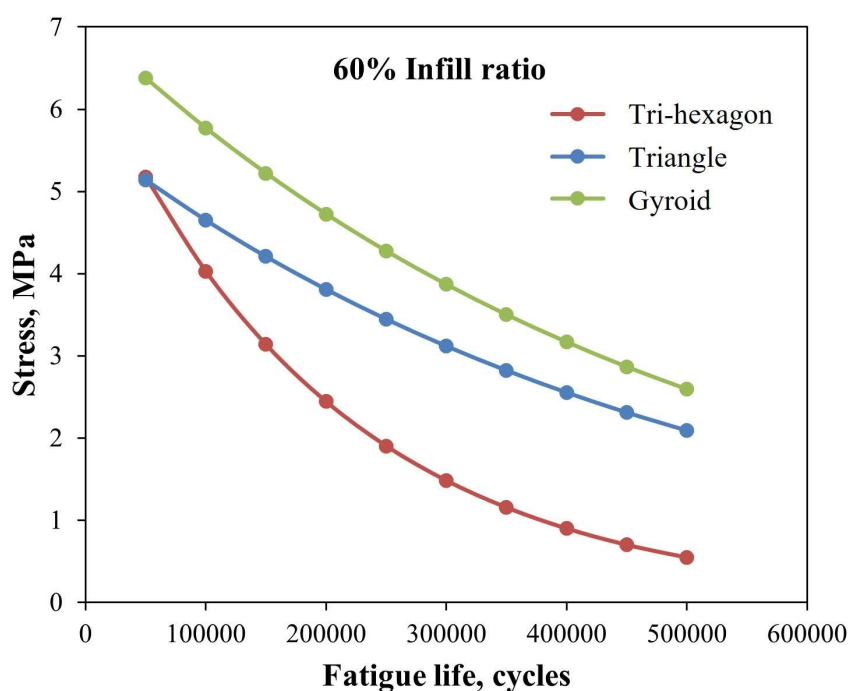
**Table 4.** Results of impact test and fracture toughness.

Specimen code	Uc (joules)	Kc (MPa·m <sup>1/2</sup> )
G 30	6.1364	3749.742668
G 60	7.8032	6368.050172
G 90	11.697	10695.37909
TR 30	6.4266	3661.944107
TR 60	14.753	8151.477331
TR 90	17.469	12012.12675

### 3.4. Fatigue test results

The fatigue life of the carbon fiber–reinforced PLA samples was investigated using 72 specimens with three infill patterns (tri-hexagon, triangle, and gyroid) and three infill ratios (30%, 60%, and 90%). The relationship between stress and fatigue life was established through the S-N curves presented in Figures 21–23. As expected, the number of cycles to failure increased with decreasing stress levels. The gyroid pattern demonstrated the best fatigue performance, followed by the triangle and tri-hexagon patterns. At the same stress level, the gyroid pattern exhibited more than twice the number of cycles to failure compared to the tri-hexagon pattern (Figure 21).

The superior fatigue resistance of the gyroid pattern can be attributed to its continuous and smooth surface, which minimizes stress concentrations and allows for better load distribution [6,12]. The carbon fiber reinforcement further enhances fatigue performance by providing additional load-bearing capacity and delaying crack propagation [2,15].

**Figure 21.** S-N curve for three patterns with a 60% infill ratio (test results).

The infill ratio also played a significant role in the fatigue life of the samples. For all infill patterns, higher infill ratios resulted in improved fatigue resistance (Figure 21). This can be explained by the increased material density and reduced void content associated with higher infill ratios, which leads to better load transfer and resistance to crack initiation and propagation [8–10].

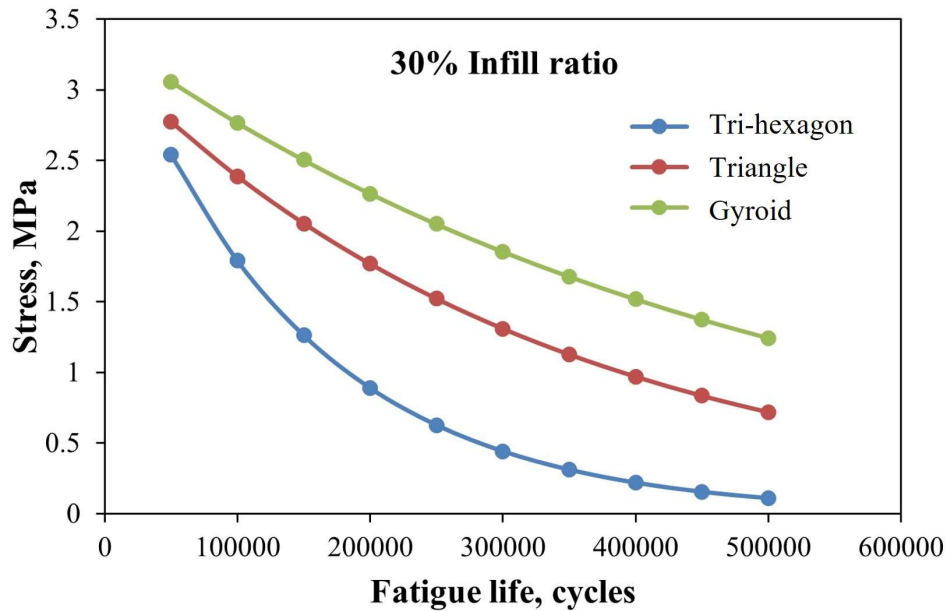


**Figure 22.** S-N curve for three patterns with a 30% infill ratio.

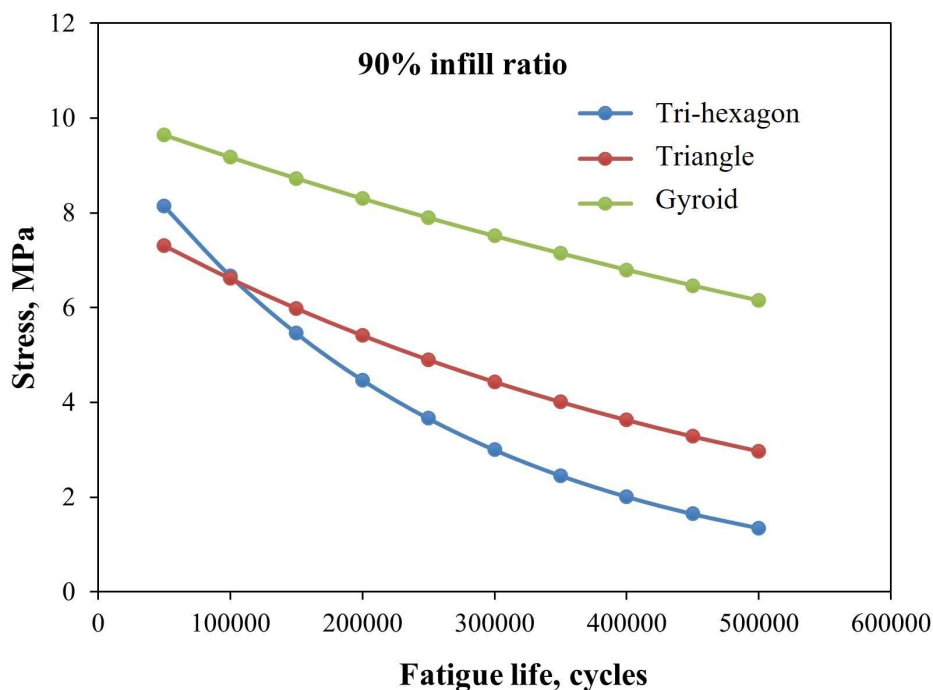


**Figure 23.** S-N curve for three patterns with a 90% infill ratio.

The infill structure, including both the pattern and ratio, plays a crucial role in determining the mechanical properties of 3D-printed parts. In this study, three infill patterns (gyroid, tri-hexagon, and triangle) and three infill ratios (30%, 60%, and 90%) were investigated. The results consistently showed that the gyroid pattern outperformed the tri-hexagon and triangle patterns in terms of tensile strength, elastic modulus, flexural modulus, and fatigue resistance. This superior performance can be attributed to the gyroid pattern's unique geometry, which features a continuous and smooth surface that allows for efficient stress distribution and minimizes stress concentrations [33].

The infill ratio also had a significant impact on the mechanical properties of the 3D-printed PLA samples. Higher infill ratios resulted in improved tensile strength, elastic modulus, and fatigue life across all infill patterns. This trend is consistent with previous studies [20–22], which have reported enhanced mechanical performance with increasing infill density. The improved properties at higher infill ratios can be explained by the increased material density and reduced void content, which facilitate better load transfer and resistance to deformation and failure [8–10].

The superior performance of the gyroid infill pattern can be attributed to several factors related to its unique geometry. First, the gyroid structure is a triply periodic minimal surface, which means it divides space into two intertwining regions with minimal surface area. This characteristic allows for a more uniform distribution of stresses throughout the structure, reducing stress concentrations that can lead to premature failure. Second, the continuous and smooth nature of the gyroid pattern provides better connectivity between layers, enhancing the overall strength and stiffness of the printed part. This improved interlayer adhesion is particularly beneficial for resisting delamination under various loading conditions. Additionally, the gyroid pattern's complex three-dimensional structure offers multiple load paths, allowing for more efficient load transfer within the material. This multi-directional load-bearing capability contributes to enhanced mechanical properties in all directions, unlike simpler infill patterns that may have preferential strength orientations. Furthermore, the gyroid structure's high surface-to-volume ratio facilitates better bonding between the infill and the outer shell of the printed part, leading to improved overall structural integrity. Lastly, the gyroid pattern's ability to maintain a consistent density throughout the part while providing a balance between material use and void space contributes to its superior performance in terms of strength-to-weight ratio.

While our study did not include direct comparisons with pure PLA samples, we can contextualize our results with those reported in the literature for PLA. For instance, Tymrak et al. [12] reported tensile strengths for 3D-printed PLA ranging from 28.5 to 52.3 MPa, depending on print parameters. In comparison, our CF-PLA samples with a 90% gyroid infill pattern achieved a tensile strength of 18.2 MPa. Although this value is lower than some reported for pure PLA, it is important to note that our study focused on different infill patterns and ratios, which significantly affect mechanical properties. Similarly, for elastic modulus, Tymrak et al. reported values ranging from 1.28 to 3.12 GPa for PLA. Our CF-PLA samples with a 90% gyroid infill pattern achieved a modulus of 999 MPa (0.999 GPa). While this is lower than some reported PLA values, it is crucial to consider the impact of infill patterns and ratios on these properties. These comparisons highlight the complex interplay between material composition, infill patterns, and infill ratios in determining the mechanical properties of 3D-printed structures. Our results demonstrate that CF-PLA can achieve significant mechanical performance, though direct comparisons with PLA would require matched printing parameters and infill structures.

The incorporation of carbon fiber reinforcement into the PLA matrix further enhanced the mechanical properties of the 3D-printed samples. The carbon fibers, with their high strength and stiffness, serve as a load-bearing framework within the PLA matrix, improving the overall strength

and rigidity of the composite material [34,35]. The reinforcing effect of the carbon fibers is particularly evident in the tensile and fatigue tests, where the CF-PLA samples exhibited significantly higher strength and fatigue life compared to unreinforced PLA propagation [36,37]. The carbon fibers also contribute to the improved impact resistance and fracture toughness of the samples by providing additional energy dissipation mechanisms and delaying crack propagation [38]. To provide a comprehensive comparison of the current work with previous studies, Table 5 presents the key findings of this research alongside those of other relevant investigations.

**Table 5.** Comparison of the current work with previous studies on 3D-printed PLA and CF-PLA composites.

Study	Material	Infill pattern and ratio	Key findings
Current work	CF-PLA	Gyroid, tri-hexagon, triangle; 30%, 60%, 90%	Gyroid pattern exhibited the best mechanical properties. Higher infill ratios improved performance. CF reinforcement enhanced strength and toughness.
Dogru et al. [39]	PLA	Honeycomb, rectilinear; 20%, 50%, 80%	Honeycomb pattern showed higher strength and stiffness. Increasing infill ratio improved properties.
Kumar et al. [40]	CF-PLA	Rectangular, triangular, honeycomb; 20%, 60%, 100%	Triangular pattern had the best mechanical performance. CF reinforcement significantly enhanced properties.
Dong et al. [41]	PLA; CF-PLA	Gyroid, grid, triangle; 25%, 50%, 75%	Gyroid pattern showed superior mechanical properties for both PLA and CF-PLA. CF reinforcement improved strength and modulus.
Lie et al. [42]	PLA; CF-PLA	Honeycomb, rectilinear, gyroid; 20%, 40%, 60%, 80%	Gyroid pattern demonstrated the highest strength and modulus for both PLA and CF-PLA. CF reinforcement led to significant improvements in mechanical properties.
Wang et al. [37]	PLA; CF-PLA	Grid, triangle, honeycomb; 30%, 50%, 70%, 90%	Triangle pattern exhibited the best mechanical performance for both materials. Higher infill ratios and CF reinforcement resulted in enhanced strength, modulus, and impact resistance.

The comparative analysis of the current work with previous studies highlights the significant influence of infill pattern, infill ratio, and carbon fiber reinforcement on the mechanical properties of 3D-printed PLA and CF-PLA composites. The gyroid infill pattern consistently demonstrates superior mechanical performance compared with other patterns, such as honeycomb, rectilinear, and triangular, in multiple studies [28,30,31]. However, some investigations have found the triangular pattern to exhibit the best mechanical properties [29,32], indicating that the optimal infill pattern may depend on the specific material and printing conditions.

Across all studies, increasing the infill ratio leads to improved mechanical properties, such as strength, stiffness, and impact resistance. This trend is attributed to the increased material density and reduced void content at higher infill ratios, which facilitate better load transfer and resistance to



deformation and failure. The incorporation of carbon fiber reinforcement is consistently shown to significantly enhance the mechanical properties of 3D-printed PLA parts. CF-PLA composites exhibit higher strength, modulus, and toughness compared to unreinforced PLA, as demonstrated in the current work and previous studies [29–32]. The reinforcing effect of carbon fibers is attributed to their high strength and stiffness, as well as their ability to serve as a load-bearing framework within the PLA matrix.

In conclusion, this comparative analysis provides valuable insights into the factors influencing the mechanical properties of 3D-printed PLA and CF-PLA composites. The findings contribute to the growing body of knowledge on additive manufacturing and material science, offering practical guidelines for designing and fabricating high-performance 3D-printed structures. The current work, in conjunction with previous studies, highlights the potential of optimizing infill patterns and ratios and incorporating carbon fiber reinforcement to enhance the mechanical performance of 3D-printed parts for various applications.

#### 4. Conclusions

In conclusion, this comparative analysis provides valuable insights into the factors influencing the mechanical properties of 3D-printed PLA and CF-PLA composites. The findings contribute to the growing body of knowledge on additive manufacturing and material science, offering practical guidelines for designing and fabricating high-performance 3D-printed structures. The current work, in conjunction with previous studies, highlights the potential of optimizing infill patterns and ratios and incorporating carbon fiber reinforcement to enhance the mechanical performance of 3D-printed parts for various applications. The present study deals with the fatigue properties and fracture toughness of 3D-printed carbon fiber-reinforced PLA samples and the effects of the infill pattern with their respective infill ratios. The experiments were designed for three infill patterns—gyroid, tri-hexagon, and triangle—and three infill ratios—30%, 60%, and 90%. The designs were tested in tensile, bending, impact, and fatigue tests. The repeatable outcomes were that the gyroid infill pattern performed better than the tri-hexagon and triangle regarding mechanical properties. The gyroid pattern's geometry is unique; it has a continuous smooth surface that could effectively distribute the stresses over the structure and lessen the stress concentration. The ultimate tensile strength was enhanced by 63% for the gyroid pattern compared with the tri-hexagon pattern, with 113% more fatigue life with a 90% infill ratio. At the same infill ratio, the gyroid pattern showed 58% higher ultimate tensile strength than the triangle pattern and 100% greater fatigue life.

In the case of 3D-printed CF-PLA samples, the influence of the infill ratio was also significant on the resulting mechanical properties. By increasing the infill ratio from 30% to 60%, it was possible to obtain an increase of 82% in ultimate tensile strength for the gyroid pattern. In comparison, the additional increment from 60% to 90% showed 90% enhancement. The tri-hexagon pattern was more sensitive to the infill ratio, where a sample with a 90% infill ratio demonstrated 113% higher ultimate tensile strength than a sample with a 60% infill ratio.

The great advantage of applying carbon fiber reinforcement in the PLA matrix relates to significantly improving its mechanical properties in the 3D-printed samples. The CF-PLA composites were found to have a much higher strength, stiffness, and toughness compared to unreinforced PLA. This reinforcing effect by carbon fibers was effectively reflected in the tensile and fatigue tests, where the CF-PLA samples showed significantly higher strength and fatigue life than those of unreinforced

PLA. Comparison of the present work with earlier investigations on PLA, as well as on CFPLA, 3D-printed composites, has always been consistent in that the gyroid infill pattern provides better mechanical results compared to honeycomb, rectilinear, and triangular patterns. Improvement of mechanical properties due to increasing infill percentage was reported in several works. On the other hand, research findings and some published work stated that there was an apparent increase in strength, stiffness, and toughness for 3D-printed PLA parts when reinforced with carbon fiber.

Results from the present work are valuable and have been a significant addition to state-of-the-art additive manufacturing and materials science, providing new insights into factors influencing the mechanical properties of 3D-printed PLA and CF-PLA composites. This will open further prospects for the fabrication of high-performance structures that can be employed in the aerospace, automotive, and biomedical engineering fields through patterns, infill ratios, and reinforcement of carbon fiber optimization.

Future research could also focus on the in-depth study of mechanisms showing the outperformance of the gyroid infill pattern or how reinforcing carbon fibers interact in a 3D-printed composite. The survey of mechanical property investigation between other parameters together with the addition of other fillers will further optimize the 3D printing process of CF-PLA composites.

This study demonstrates that significant improvement in the fatigue properties and fracture toughness of 3D-printed PLA parts can be obtained by optimizing infill patterns and ratios and by including carbon fiber reinforcement. The gyroid infill pattern at high ratios and with carbon fiber reinforcement gave the best mechanical performance, showing improvements of 58% to 113% compared to other infill patterns and lower ratios. This opens up a practical guideline for designing and fabricating high-performance 3D-printed structures by using CF-PLA composites, which paves the way for an ultimate mass application of the additive manufacturing technique in different engineering fields.

### **Use of AI tools declaration**

The authors declare they have not used Artificial Intelligence (AI) tools in the creation of this article.

### **Author contributions**

Lubna Layth Dawood: conceptualization, methodology, software, formal analysis, investigation, data curation, writing—original draft, writing—review & editing, visualization. Ehsan Sabah AlAmeen: conceptualization, methodology, validation, resources, writing—review & editing, supervision, project administration.

### **Acknowledgments**

The authors wish to thank Mustansiriyah University (College of Engineering) of facilities in their labs.

### **Conflict of interest**

The authors declare no conflict of interest.

## References

- 1 Ayatollahi MR, Nabavi-Kivi A, Bahrami B, et al. (2020) The influence of in-plane raster angle on tensile and fracture strengths of 3D-printed PLA specimens. *Eng Fract Mech* 237: 107225. <https://doi.org/10.1016/j.engfracmech.2020.107225>
- 2 Ogaili AAF, Basem A, Kadhim MS, et al. (2024) The effect of chopped carbon fibers on the mechanical properties and fracture toughness of 3D-printed PLA parts: An experimental and simulation study. *J Compos Sci* 8: 273. <https://doi.org/10.3390/jcs8070273>
- 3 Vălean E, Foti P, Razavi SMJ, et al. (2023) Static and fatigue behavior of 3D printed PLA and PLA reinforced with short carbon fibers. *J Mech Sci Technol* 37: 5555–5559. <https://doi.org/10.1007/s12206-023-0822-2>
- 4 Ogaili AAF, Jaber AA, Hamzah MN (2023) Wind turbine blades fault diagnosis based on vibration dataset analysis. *Data Brief* 49: 109414. <https://doi.org/10.1016/j.dib.2023.109414>
- 5 Simmons H, Tiwary P, Colwell JE, et al. (2019) Improvements in the crystallinity and mechanical properties of PLA by nucleation and annealing. *Polym Degrad Stab* 166: 248–257. <https://doi.org/10.1016/j.polyimdegradstab.2019.05.036>
- 6 Kumar Patro P, Kandregula S, Suhail Khan MN, et al. (2023) Investigation of mechanical properties of 3D printed sandwich structures using PLA and ABS. *Mater Today Proc.* <https://doi.org/10.1016/j.matpr.2023.08.366>
- 7 Ogaili AAF, Jaber AA, Hamzah MN (2023) A methodological approach for detecting multiple faults in wind turbine blades based on vibration signals and machine learning. *Curved Layer Struct* 10: 20220214. <https://doi.org/10.1515/cls-2022-0214>
- 8 Jap NSF, Pearce GM, Hellier AK, et al. (2019) The effect of raster orientation on the static and fatigue properties of filament deposited ABS polymer. *Int J Fatigue* 124: 328–337. <https://doi.org/10.1016/j.ijfatigue.2019.03.018>
- 9 Dizon JRC, Espera AH, Chen Q, et al. (2018) Mechanical characterization of 3D-printed polymers. *Addit Manuf* 20: 44–67. <https://doi.org/10.1016/j.addma.2017.12.002>
- 10 Popescu D, Zapciu A, Amza C, et al. (2018) FDM process parameters influence over the mechanical properties of polymer specimens: A review. *Polym Test* 69: 157–166. <https://doi.org/10.1016/j.polymertesting.2018.05.020>
- 11 Chacón JM, Caminero MA, García-Plaza E, et al. (2017) Additive manufacturing of PLA structures using fused deposition modelling: Effect of process parameters on mechanical properties and their optimal selection. *Mater Design* 124: 143–157. <https://doi.org/10.1016/j.matdes.2017.03.065>
- 12 Rezanezhad S, Azadi M (2024) The influence of 3D-printed PLA coatings on pure and fretting fatigue properties of AM60 magnesium alloys under cyclic bending loads. *Heliyon* 10: e29552. <https://doi.org/10.1016/j.heliyon.2024.e29552>
- 13 Rodríguez-Panes A, Claver J, Camacho AM (2018) The influence of manufacturing parameters on the mechanical behaviour of PLA and ABS pieces manufactured by FDM: A comparative analysis. *Materials* 11: 1333. <https://doi.org/10.3390/ma11081333>
- 14 Tymrak BM, Kreiger M, Pearce JM (2014) Mechanical properties of components fabricated with open-source 3-D printers under realistic environmental conditions. *Mater Design* 58: 242–246. <https://doi.org/10.1016/j.matdes.2014.02.038>

15. Sajjadi SA, Ashenai Ghasemi F, Rajaei P, et al. (2022) Evaluation of fracture properties of 3D printed high impact polystyrene according to essential work of fracture: Effect of raster angle. *Addit Manuf* 59: 103191. <https://doi.org/10.1016/j.addma.2022.103191>
16. Karimi HR, Khedri E, Nazemzadeh N, et al. (2023) Effect of layer angle and ambient temperature on the mechanical and fracture characteristics of unidirectional 3D printed PLA material. *Mater Today Commun* 35: 106174. <https://doi.org/10.1016/j.mtcomm.2023.106174>
17. Ganeshkumar S, Kumar SD, Magarajan U, et al. (2022) Investigation of tensile properties of different infill pattern structures of 3D-printed PLA polymers: Analysis and validation using finite element analysis in ANSYS. *Materials* 15: 5142. <https://doi.org/10.3390/ma15155142>
18. Srinivasan R, Ruban W, Deepanraj A, et al. (2020) Effect on infill density on mechanical properties of PETG part fabricated by fused deposition modelling. *Mater Today Proc* 27: 1838–1842. <https://doi.org/10.1016/j.matpr.2020.03.788>
19. Casavola C, Cazzato A, Moramarco V, et al. (2016) Orthotropic mechanical properties of fused deposition modelling parts described by classical laminate theory. *Mater Design* 90: 453–458. <https://doi.org/10.1016/j.matdes.2015.11.009>
20. Domingo-Espin M, Puigoriol-Forcada JM, Garcia-Granada AA, et al. (2015) Mechanical property characterization and simulation of fused deposition modeling Polycarbonate parts. *Mater Design* 83: 670–677. <https://doi.org/10.1016/j.matdes.2015.06.074>
21. Lanzotti A, Grasso M, Staiano G, et al. (2015) The impact of process parameters on mechanical properties of parts fabricated in PLA with an open-source 3-D printer. *Rapid Prototyping J* 21: 604–617. <https://doi.org/10.1108/RPJ-09-2014-0135>
22. Gurralla PK, Regalla SP (2014) Part strength evolution with bonding between filaments in fused deposition modelling: This paper studies how coalescence of filaments contributes to the strength of final FDM part. *Virtual Phys Prototy* 9: 141–149. <https://doi.org/10.1080/17452759.2014.913400>
23. Gomez-Gras G, Jerez-Mesa R, Travieso-Rodriguez JA, et al. (2018) Fatigue performance of fused filament fabrication PLA specimens. *Mater Design* 140: 278–285. <https://doi.org/10.1016/j.matdes.2017.11.072>
24. Hu Y, Lin Y, Yang L, et al. (2024) Additive manufacturing of carbon fiber-reinforced composites: A review. *Appl Compos Mater* 31: 353–398. <https://doi.org/10.1007/s10443-023-10211-0>
25. Ogaili AAF, Al-Ameen ES, Kadhim MS, et al. (2020) Evaluation of mechanical and electrical properties of GFRP composite strengthened with hybrid nanomaterial fillers. *AIMS Mater Sci* 7: 93–102. <https://doi.org/10.3934/matserci.2020.1.93>
26. Al-Ameen ES, Al-Sabbagh MNM, Ogaili AAF, et al. (2022) Role of pre-stressing on anti-penetration properties for kevlar/epoxy composite plates. *Int J Nanoelectron Mater* 15: 293–302. Available from: <http://www.ijneam.unimap.edu.my/images/PDF/Vol15No4/IJNEAM-V15N4P1.pdf>.
27. Ogaili AAF, Hamzah MN (2022) Integration of machine learning (ML) and finite element analysis (FEA) for predicting the failure modes of a small horizontal composite blade. *IJRER* 4: 2168–2179. <https://doi.org/10.20508/ijrer.v12i4.13354.g8589>
28. Hamdan ZK, Ogaili AAF, Metteb ZW, et al. (2021) Study the electrical, thermal behaviour of (glass/jute) fibre hybrid composite material. *J Phys Conf Ser* 1783: 012070. <https://doi.org/10.1088/1742-6596/1879/1/012070>

29. Abdulla FA, Qasim MS, Ogaili AAF (2021) Influence eggshells powder additive on thermal stress of fiberglass/polyester composite tubes. *IOP Conf Ser Earth Environ Sci* 877: 012039. <https://doi.org/10.1088/1755-1315/779/1/012039>
30. Ogaili AAF, Abdulla FA, Al-Sabbagh MNM, et al. (2020) Prediction of mechanical, thermal and electrical properties of wool/glass fiber based hybrid composites. *IOP Conf Ser Mater Sci Eng* 928: 022004. <https://doi.org/10.1088/1757-899X/870/1/022004>
31. Mohammed KA, Al-Sabbagh MNM, Ogaili AAF, et al. (2020) Experimental analysis of hot machining parameters in surface finishing of crankshaft. *JMERD* 43: 105–114.
32. Cao M, Cui T, Yue Y, et al. (2023) Preparation and characterization for the thermal stability and mechanical property of PLA and PLA/CF samples built by FFF approach. *Materials* 16: 5023. <https://doi.org/10.3390/ma16145023>
33. Monaldo E, Ricci M, Marfia S (2023) Mechanical properties of 3D printed polylactic acid elements: Experimental and numerical insights. *Mech Mater* 177: 104551. <https://doi.org/10.1016/j.mechmat.2023.104551>
34. Ivey M, Melenka GW, Carey JP, et al. (2017) Characterizing short-fiber-reinforced composites produced using additive manufacturing. *Adv Manuf-Polym Comp* 3: 81–91. <https://doi.org/10.1080/20550340.2017.1341125>
35. Tian X, Liu T, Yang C, et al. (2016) Interface and performance of 3D printed continuous carbon fiber reinforced PLA composites. *Composites Part A* 88: 198–205. <https://doi.org/10.1016/j.compositesa.2016.05.032>
36. Zhang H, Yang D, Sheng Y (2018) Performance-driven 3D printing of continuous curved carbon fibre reinforced polymer composites: A preliminary numerical study. *Compos Part B-Eng* 151: 256–264. <https://doi.org/10.1016/j.compositesb.2018.06.017>
37. Wang X, Jiang M, Zhou Z, et al. (2017) 3D printing of polymer matrix composites: A review and prospective. *Compos Part B-Eng* 110: 442–458. <https://doi.org/10.1016/j.compositesb.2016.11.034>
38. Yang L, Zhou L, Lin Y, et al. (2024) Failure mode analysis and prediction model of additively manufactured continuous carbon fiber-reinforced polylactic acid. *Polym Compos* 45: 7205–7221. <https://doi.org/10.1002/pc.28261>
39. Dogru A, Sozen A, Naser G, et al. (2021) Effects of aging and infill pattern on mechanical properties of hemp reinforced PLA composite produced by fused filament fabrication (FFF). *ASEP* 14: 651–660. <https://doi.org/10.14416/j.asep.2021.08.007>
40. Kumar KR, Mohanavel V, Kiran K (2022) Mechanical properties and characterization of polylactic acid/carbon fiber composite fabricated by fused deposition modeling. *J Mater Eng Perform* 31: 4877–4886. <https://doi.org/10.1007/s11665-021-06566-7>
41. Dong G, Tang Y, Zhao YF (2017) A survey of modeling of lattice structures fabricated by additive manufacturing. *J Mech Design* 139: 100906. <https://doi.org/10.1115/1.4037305>
42. Li L, Liu W, Sun L (2022) Mechanical characterization of 3D printed continuous carbon fiber reinforced thermoplastic composites. *Compos Sci Technol* 227: 109618. <https://doi.org/10.1016/j.compscitech.2022.109618>

